Appendix A Synchrotron radiation characteristics

D. Einfeld

A.1 Introduction

Synchrotron radiation is characterized in general by the following attributes: spectral range, photon flux, photon flux density, brilliance, and polarization. The photon flux (photons per second and bandwidth) is the overall flux collected by an experiment and reaching the sample; the photon flux density is the flux per unit area at the sample; and the brilliance is the flux per unit area and opening angle. This appendix summarizes the formulas for the calculation of these quantities for the synchrotron radiation emitted from a stored beam in the bending magnet, wiggler, and undulator [A.1–A.9].

Establishing the theory of synchrotron radiation has been the work of many researchers. Today most of the calculations use the results of the Schwinger theory [A.6, A.2]. A relativistic electron moving around an orbit emits a radiation cone tangential to the orbit with a small opening cone, as shown in Fig. A.1. The aperture of the beam line of width B and height H at a distance D determines the flux that goes to the sample.

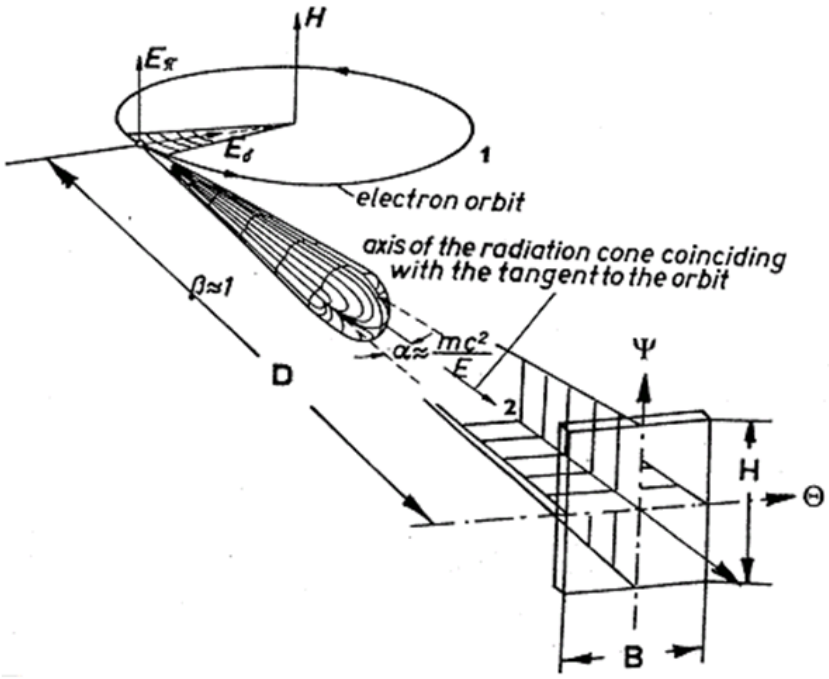

Fig. A.1: Characteristics of the synchrotron radiation emitted by a relativistic electron moving in a circle

The shape and intensity within the radiation cone, according to the Schwinger theory, is given by

$$\frac{\mathrm{d}^2\Phi}{\mathrm{d}\theta\,\mathrm{d}\psi} = \frac{3\alpha}{4\pi^2}\gamma^2\frac{\Delta\omega}{\omega}\frac{I}{e}y^2(1+X^2)\left[K_{2/3}^2(\xi)+\frac{X^2}{1+X^2}K_{1/3}^2(\xi)\right], \tag{A.1}$$

where:

Φ is the photon flux (number of photons per second);

θ is the observation angle in the horizontal plane;

ψ is the observation angle in the vertical plane;

α is the fine structure constant (equal to 1/137);

γ is the electron energy ($m_e c^2$ where m_e is the electron mass and c is the velocity of light);

https://doi.org/10.23731/CYRM-2020-001.171

ω is the angular frequency of photons ($h\omega$ = photon energy = ε);

I is the beam current;

e is the electron charge (1.601×10^{-19} C);

$y = \omega/\omega_c = \varepsilon/\varepsilon_c$ (where ω_c is the critical frequency, $3\gamma 3c/2\rho$);

E_c is the critical photon energy ($3hc\gamma\ 3/2\rho$);

ρ is the radius of instantaneous curvature of the electron trajectory (E/ecB in practical units, ρ[m] = $3.3356 \times (E/\text{GeV})/(B/\text{T})$);

c is the speed of light (2.9979×10^8 m/s);

E is the electron beam energy;

B is the magnetic field strength;

$\varepsilon_c = h\omega_c$ (ε_c[keV] = $0.665 \times (E/\text{GeV})^2 \times (B/\text{T})$);

$X = \gamma\psi$ (normalized angle in the vertical plane);

$\xi = y(1+X^2)3/2/2$.

The subscripted K's in equation (A.1) are modified Bessel functions of the second kind. Equation (A.1) is the basic formula for the calculation of synchrotron radiation characteristics. The polarization is given by the two terms within the square brackets.

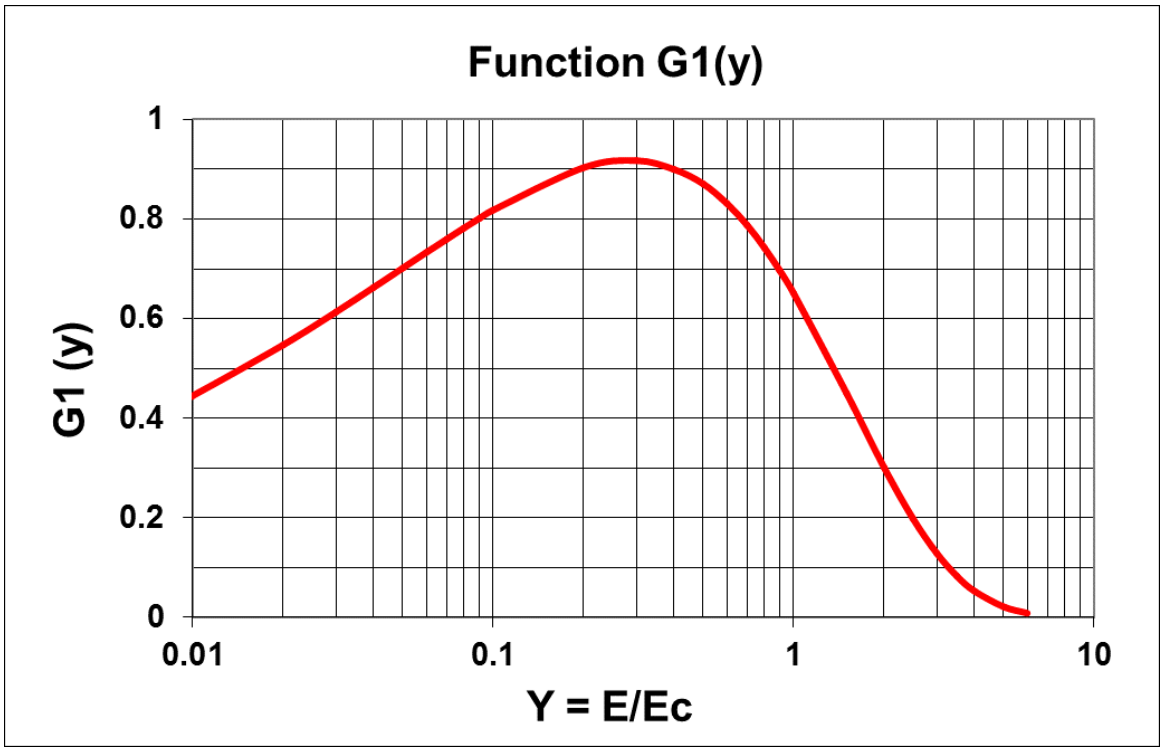

Fig. A.2: The parameter G_1 as a function of the normalized photon energy $\varepsilon/\varepsilon_c$

For synchrotron radiation users, three parameters are important (see Fig. A.1):

– the 'photon flux', i.e. the numbers of photons per second and per unit band width;

– the 'photon flux density', which is the photon flux divided by the beam cross-section, i.e. flux density = flux/A_s [photons/(s mm^2 BW)].

– the 'brilliance', which is the flux density divided by the opening angles $\Delta\theta$ and $\Delta\psi$, i.e. brilliance = flux density/($\Delta\theta\Delta\psi$) [photons/(s mm^2 mrad^2 BW)].

A.2 Radiation from a bending magnet

The photon flux of the synchrotron radiation from the bending magnet as a function of the horizontal opening angle is given by

$$\frac{\mathrm{d}\Phi(y)}{\mathrm{d}\theta} = 2.458\times10^{13}\,\frac{\text{photons}}{s\cdot 0.1\%\text{BW}\cdot\text{mrad}}\,(E/\text{GeV})(I/\text{A})(\theta/\text{mrad})\cdot G_1\left(\frac{\varepsilon}{\varepsilon_\text{c}}\right). \qquad \text{(A.2)}$$

According to Eq. (A.2), the photon flux is proportional to the beam current, the energy and the normalized function $G_1(\varepsilon/\varepsilon_\text{c})$, which depends only on the critical photon energy (see Fig. A.2). The equation for the critical photon energy ε_c is

$$\varepsilon_\text{c} = 0.655\,\text{keV}\cdot(E/\text{GeV})^2(B/\text{T})\,. \qquad \text{(A.3)}$$

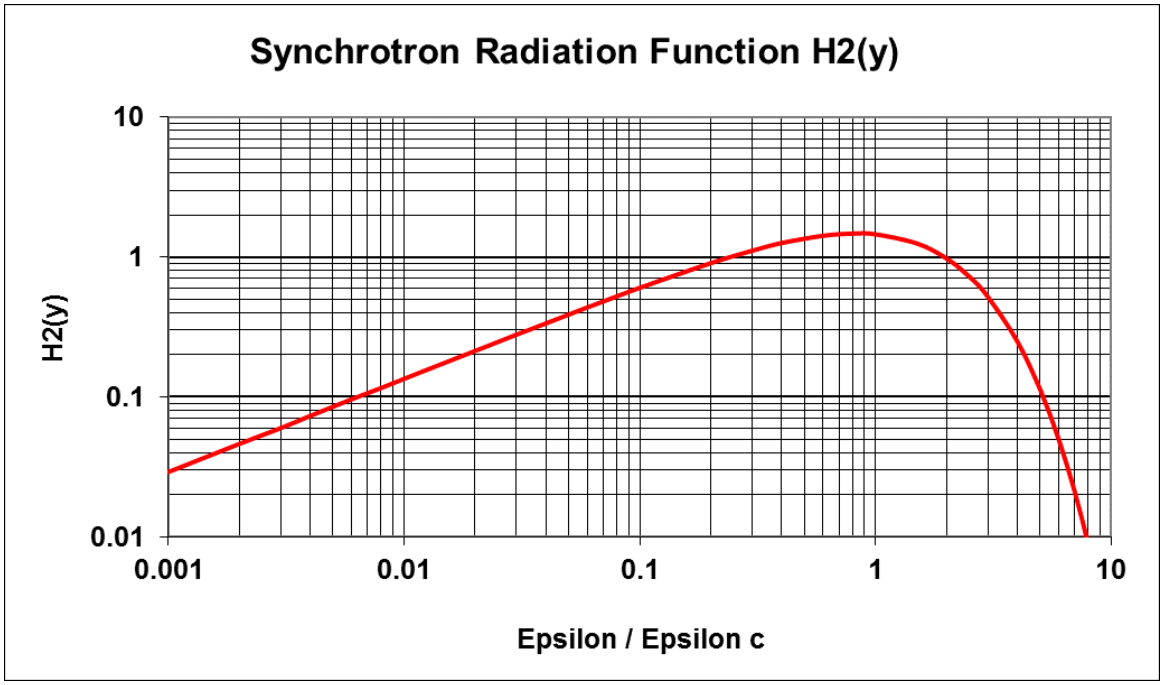

Fig. A.3: The parameter H_2 as a function of the normalized photon energy $\varepsilon/\varepsilon_\text{c}$

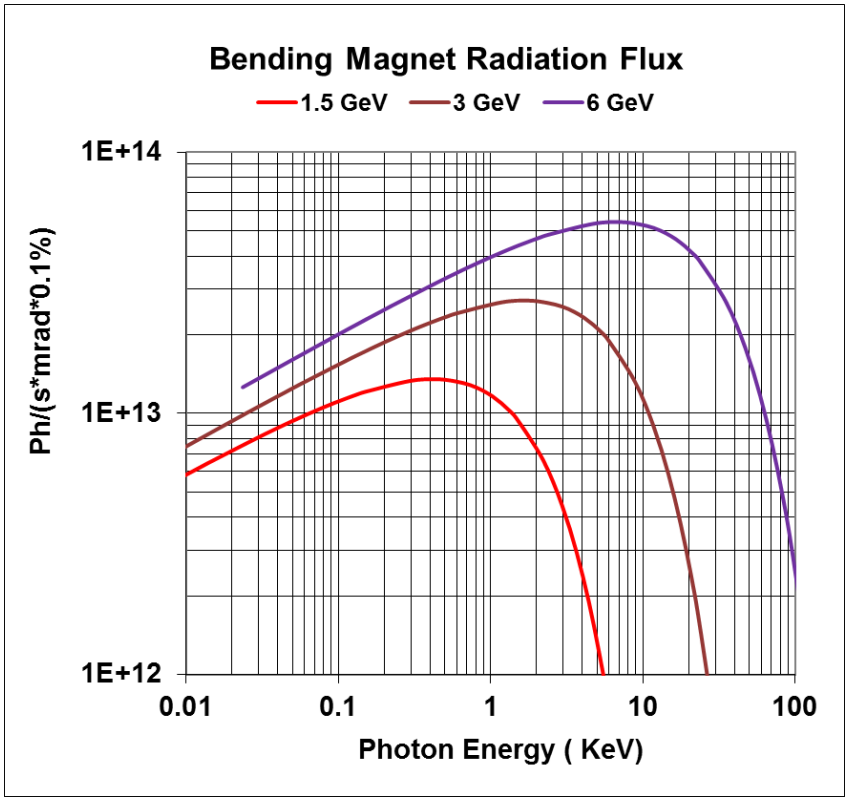

Fig. A.4: The photon flux emitted within the bending magnets for different electron energies (1.5 GeV, 3 GeV, and 6 GeV) and a current of 500 mA.

The intensity of the synchrotron radiation in the middle of the radiation cone ($\theta = 0$ and $\psi = 0$) is given by the following formula (central intensity):

$$\frac{\mathrm{d}^2\Phi(y)}{\mathrm{d}\theta\,\mathrm{d}\psi} = 1.326\times10^{13}\,\frac{\text{photons}}{s\cdot 0.1\%\cdot\theta\,\text{mrad}\cdot\psi\,\text{mrad}}\,(E/\text{GeV})^2(I/\text{A})\cdot H_2\left(\frac{\varepsilon}{\varepsilon_\text{c}}\right). \qquad \text{(A.4)}$$

The normalized function $H_2(\varepsilon/\varepsilon_\text{c})$ is presented in Fig. A.3.

The photon flux as a function of the emitted photon energy for different beam energies (1.5 GeV, 3 Gev, and 6 GeV and a field of 1 T) is presented in Fig. A.4. The photon flux increases with the beam energy. In order to cover the soft-X-ray region (approximately 6–10 keV), beam energies of 1.5–2 GeV are needed. To reach the hard-X-ray region, the beam energy has to be 3–4 GeV. To reach photon energies of up to 100 keV, a beam energy of roughly 6 GeV is required.

Some users will be interested in the photon flux density (see Fig. A.5), which is the photon flux divided by the cross-section of the stored electron beam, because the cross-section of the beam will be imaged on the sample. With beam dimensions of $\sigma(x) = 11.3$ µm and $\sigma(y) = 3.2$ µm in the middle of the bending, the flux density should be around four orders of magnitudes higher than the flux, going from 10^{13} to 10^{17}–10^{18}.

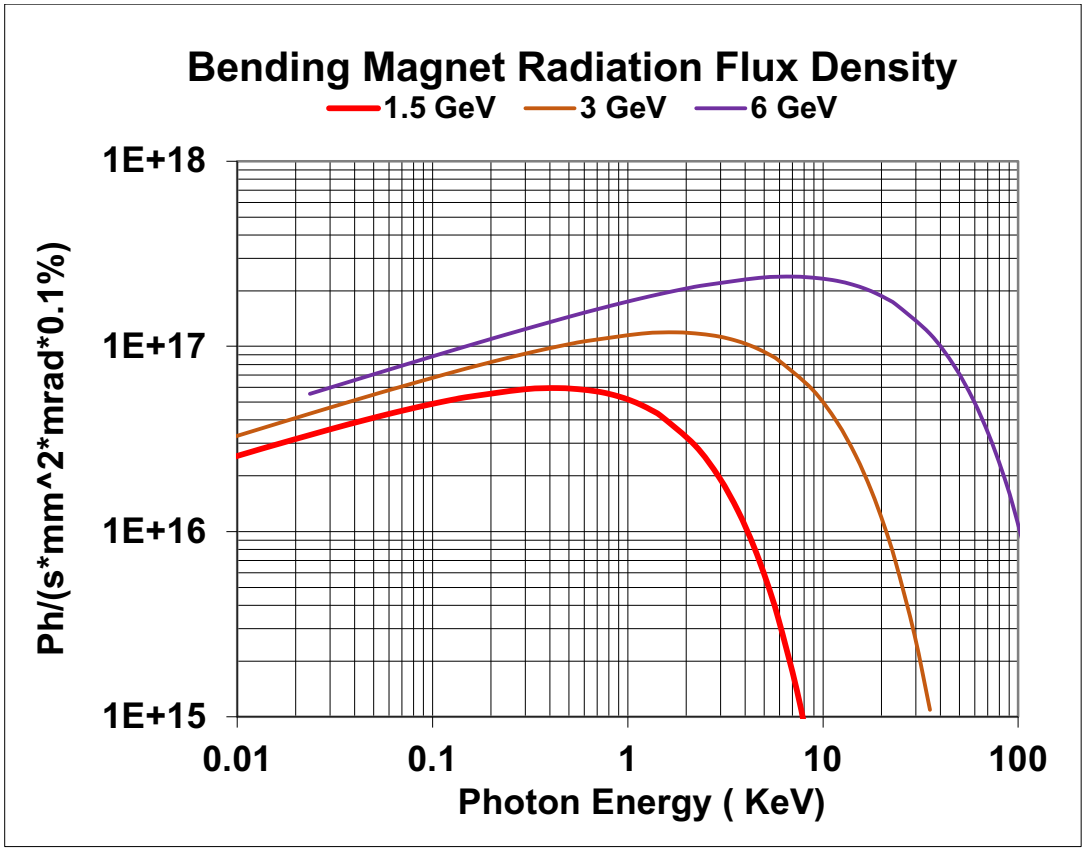

Fig. A.5: The photon flux density (for beam dimensions $\sigma(x)$ = 11.3 μm and $\sigma(y)$=3.2 μm) emitted from the bending magnet of SEE-LS at different energies and a current of 400 mA.

Because the radiation cone gets narrower with higher energy, the central intensity is proportional to the square of the energy. The spectral dependency is given by the normalized synchrotron function $H_2(y) = H_2(\varepsilon/\varepsilon_c)$. From the definition of the flux (Eq. (A.1)) and the central intensity (Eq. (A.4)), the vertical opening angle of the synchrotron radiation is given by

$$\sigma_\psi = \frac{1}{\sqrt{2\pi}} \cdot \frac{\left\langle \frac{\mathrm{d}\Phi}{\mathrm{d}\theta} \right\rangle}{\left\langle \frac{\mathrm{d}^2\Phi}{\mathrm{d}\theta\,\mathrm{d}\psi} \right\rangle}(\psi = 0) = \sqrt{\frac{2\pi}{3}} \cdot \frac{1}{\gamma} \cdot \frac{G_1(y)}{H_2(y)} = 0.7395\ \mathrm{mrad} \cdot \frac{1}{E/\mathrm{GeV}} \cdot \frac{G_1(y)}{H_2(y)}\ . \qquad \text{(A.5)}$$

The opening angle of the synchrotron radiation from the bending magnet of SEE-LS for a stored beam with different energies is presented in Fig. A.6.

The opening angle at the critical photon energy (y =1 or $\varepsilon = \varepsilon_c$) is, according to Eq. (A.5),

$$\sigma_\psi(y=1) = 0.331\ \mathrm{mrad} \cdot \frac{1}{E/\mathrm{GeV}}\ . \qquad \text{(A.6)}$$

For a 3.0 GeV machine the corresponding angle is 0.11 mrad.

Most users would be interested in the photon brilliance. The brilliance of the synchrotron radiation from a bending magnet is given by the central intensity divided by the cross-section of the beam:

$$\mathrm{Br} = \frac{\left\langle \frac{\mathrm{d}^2\Phi}{\mathrm{d}\theta\,\mathrm{d}\psi} \right\rangle(\psi = 0)}{2\pi\,\Sigma_x\Sigma_y}\ , \qquad \text{(A.7)}$$

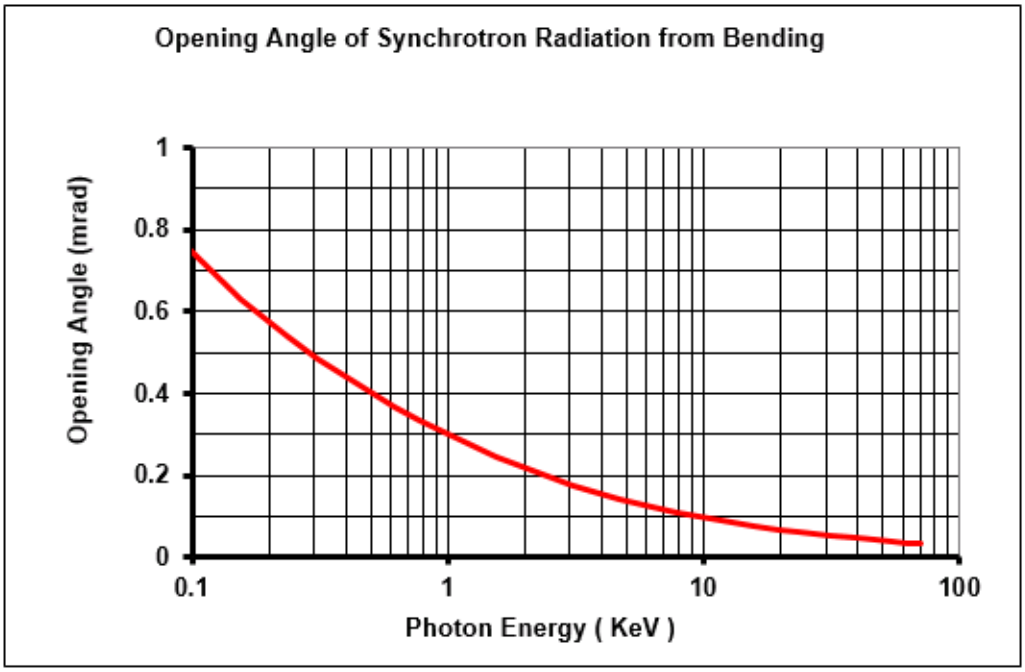

Fig. A.6: Opening angle of the synchrotron radiation from the bending magnet at 2.5 Ge.V

with

$$\Sigma_x = \left[\varepsilon_x\beta_x + \eta_x^2\sigma_E^2 + \sigma_r^2\right]^{1/2}, \quad \Sigma_y = \left[\varepsilon_y\beta_y + \sigma_r^2 + \frac{\varepsilon_y^2 + \varepsilon_y\gamma_y\sigma_r^2}{\sigma_\psi^2}\right]^{1/2}, \tag{A.8}$$

where

ε_x (ε_y) is the electron beam emittance in the horizontal (vertical) plane;

β_x (β_y) is the electron beam beta function in the horizontal (vertical) plane;

η_x is the dispersion function in the horizontal plane;

$\sigma_{E:}$ is the r.m.s. value of the relative energy spread;

γ_y is the Twiss parameter in the vertical plane;

σ_ψ is the r.m.s. value of the radiation opening angle;

$\sigma_r = \lambda/(4\pi\sigma_\psi)$ is the diffraction-limited source size;

λ is the observed photon wavelength.

At a photon energy of 10 keV the corresponding photon wavelength is 0.124 nm and the opening angle is smaller than 0.1 mrad (see Fig. A.6). This results in a diffraction-limited source size of σ_r = 1.24 µm. The term $\varepsilon_y/\sigma_\psi$ gives a cross-section of 2 µm, and $\varepsilon_y\gamma_y/\sigma_\psi^2$ has a value between 1×10^{-3} and 4×10^{-3}. These factors are at least one order of magnitude smaller than the beam cross-section sizes σ_x and σ_y; hence the overall cross-sections in Eq. (A.8) reduce to

$$\Sigma_x = \left[\varepsilon_x\beta_x + \eta_x^2\sigma_E^2\right]^{1/2}, \quad \Sigma_y = \left[\varepsilon_y\beta_y\right]^{1/2}, \tag{A.9}$$

and the brilliance of the synchrotron radiation from the bending magnet of a non-diffraction-limited light source is given by

$$\mathrm{Br}_{\mathrm{Magnet}} = \frac{\left\langle \frac{\mathrm{d}^2\Phi}{\mathrm{d}\theta\,\mathrm{d}\psi} \right\rangle (\psi = 0)}{2\pi \left[\varepsilon_x \beta_x + \eta_x^2 \sigma_E^2 \right]^{1/2} \left[\varepsilon_y \beta_y \right]^{1/2}} = \frac{\left\langle \frac{\mathrm{d}^2\Phi}{\mathrm{d}\theta\,\mathrm{d}\psi} \right\rangle (\psi = 0)}{2\pi\, \sigma_x \sigma_y} \,. \tag{A.10}$$

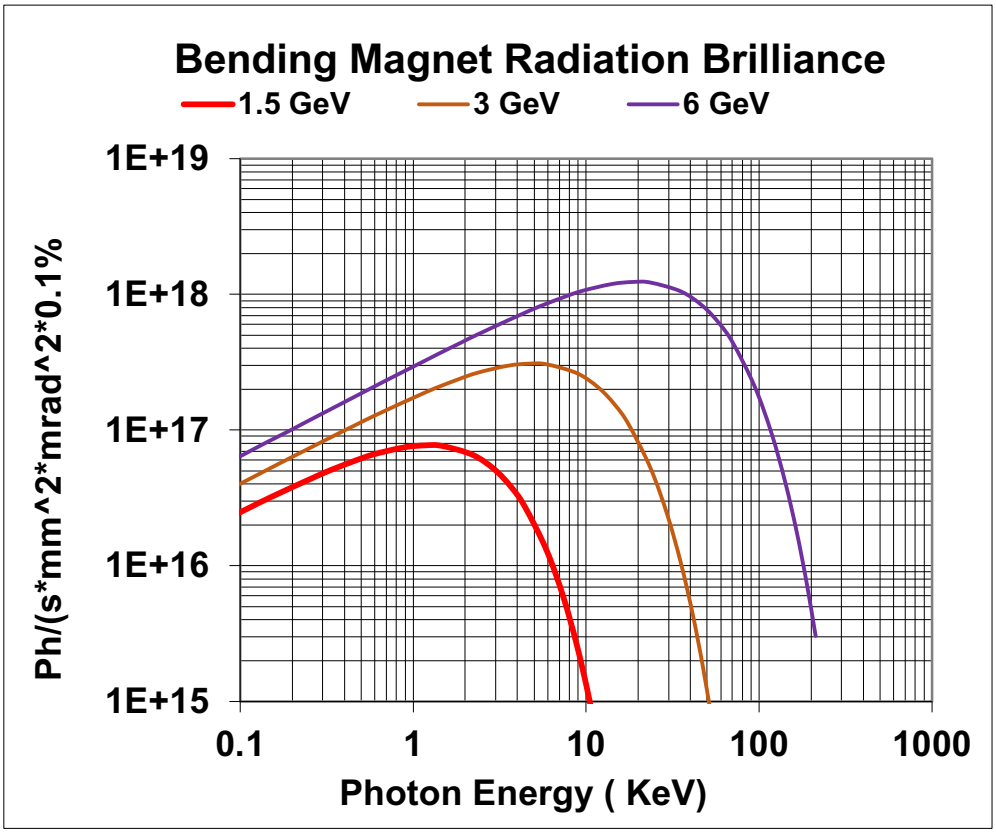

Fig. A.7: Radiation brilliance from the bending magnet at different energies, a current of 400 mA, and a field of 1 T.

Plots of the brilliance of the synchrotron radiation emitted from the bending magnets (for I = 500 mA and B =1 T) at different energies are presented in Fig. A.7. The brilliance, as well the spectrum, increases with the energy of the beam.

A.3 Radiation from a wiggler

The wiggler is a special magnet with alternating directions of the magnetic field, and the trajectory of an electron beam through a wiggler is like a snake—a sinusoidal oscillation with the peak field in the middle of the magnets [A.4, A.5]. The arrangement of the magnets in a so-called 'hybrid design' (HYB) is shown in Fig. A.8. The arrows symbolize the direction of the magnetic field in the different materials. The green and yellow blocks are special permanent magnets, and the brown blocks are made of magnetic steel. The trajectory of the electron beam in such a wiggler is presented in Fig. A.9 (blue line). The red arrows symbolize the emitted radiation, and it follows that an overlapping of the radiation cone will occur. With this arrangement of magnets, the photon flux, flux density, and brilliance will increase approximately with the number of poles. The electron beam in the wiggler has a maximum amplitude X_0 and a maximum slope X_0'.

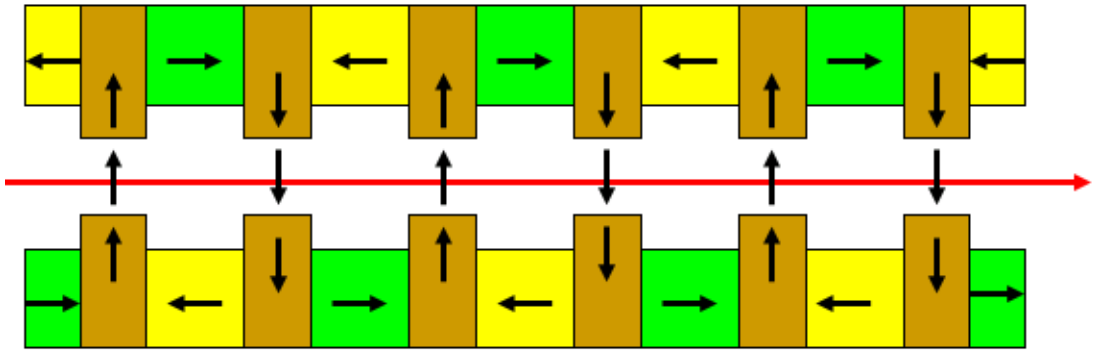

Fig. A.8: The arrangement of magnets within a wiggler; the green and yellow blocks represent permanent magnets, and the brown blocks are made of magnetic steel.

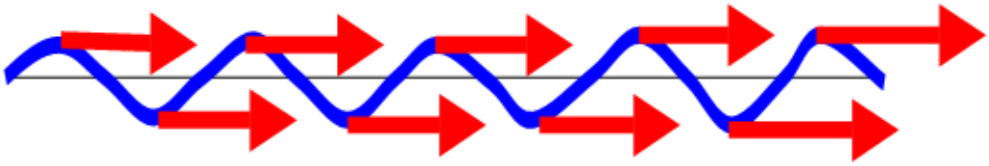

Fig. A.9: The trajectory of an electron beam within a wiggler (blue line); the red arrows symbolize the emitted synchrotron radiation in the horizontal direction.

The maximum slope X_0' and the maximum amplitude X_0 characterize the trajectory of the electron beam. They are given by

$$X_0 = \frac{1}{2\pi}\cdot\frac{K}{\gamma}\cdot\lambda_\mathrm{p} = \frac{8.13\times10^{-5}}{(E/\mathrm{GeV})}K\lambda_\mathrm{p}, \quad X_0' = \frac{K}{\gamma}, \quad K = 0.934(B/\mathrm{T})(\lambda_\mathrm{p}/\mathrm{cm})\ . \tag{A.11}$$

The photon flux, as well as the central intensity of the radiation emitted by the wiggler, is the same as from the bending magnet but a factor of N_p more intense, where N_p is the number of poles within the wiggler. The value of N_p is, according to Table A.1, 86 (twice N_per). For the synchrotron radiation from the wigglers, the critical energy ε_c determines everything. To reach the same spectral range as from the bending magnets (given by ε_c; see Eq. (A.3)), the magnetic flux density within the wigglers must be the same as within the bending magnets or—for shifting the spectrum to higher photon energies—even higher. At CCRL, Daresbury Laboratory, UK, fields of up to 2.5 T can be attained with 'hybrid design'. Higher fields are possible with superconducting devices; at the MAX IV Laboratory, Lund, Sweden, fields of up to 3 T can be reached. In Table A.1 the data needed for calculation of the wiggler radiation characteristics at the different energies are summarized.

Table A.1: Parameters for the calculation of the wiggler radiation characteristics

Energy	Unit	1.5 GeV	3 GeV	6 GeV
Current	mA	500	500	200
Field	T	3.7	3.7	3.7
L period	mm	46	46	46
N periods		43	43	43
K value		15.88	15.88	15.88
Emittance *x*	pmrad	64.1	251	1005
Emittance *y*	pmrad	5	5	5
σ_x	μm	31	62	124
σ_y	μm	4.7	4.7	4.7
β_x		15.16	15.16	15.16
β_y		4.44	4.44	4.44
Disp. *x*	m	0	0	0
Energy spread	1.0E-04	4.4	8.8	17.7
X_0	μm	39.6	19.8	9.9
X_0'	μrad	5.4	2.7	1.4

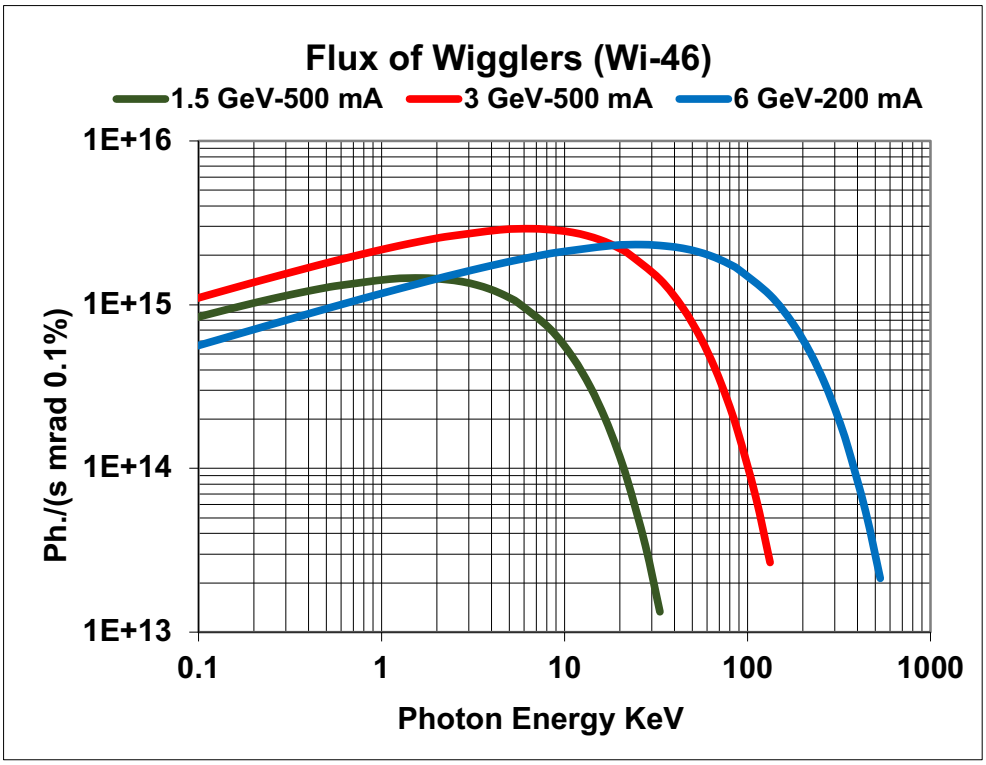

Figure A.10: The radiation flux of wiggler Wi-46 installed at SEE-LS for different energies and currents of 600 mA (1.5 GeV and 3 GeV) and 400 mA (6 GeV).

The wiggler radiation flux and flux density according to the parameters in Table A.1 are plotted in Figs. A.10 and A.11. The flux from the wiggler as a function of the photon energy has the beam characteristics of the bending magnet radiation, except that the intensity is higher by a factor 86 ($2 \times N_{per}$).

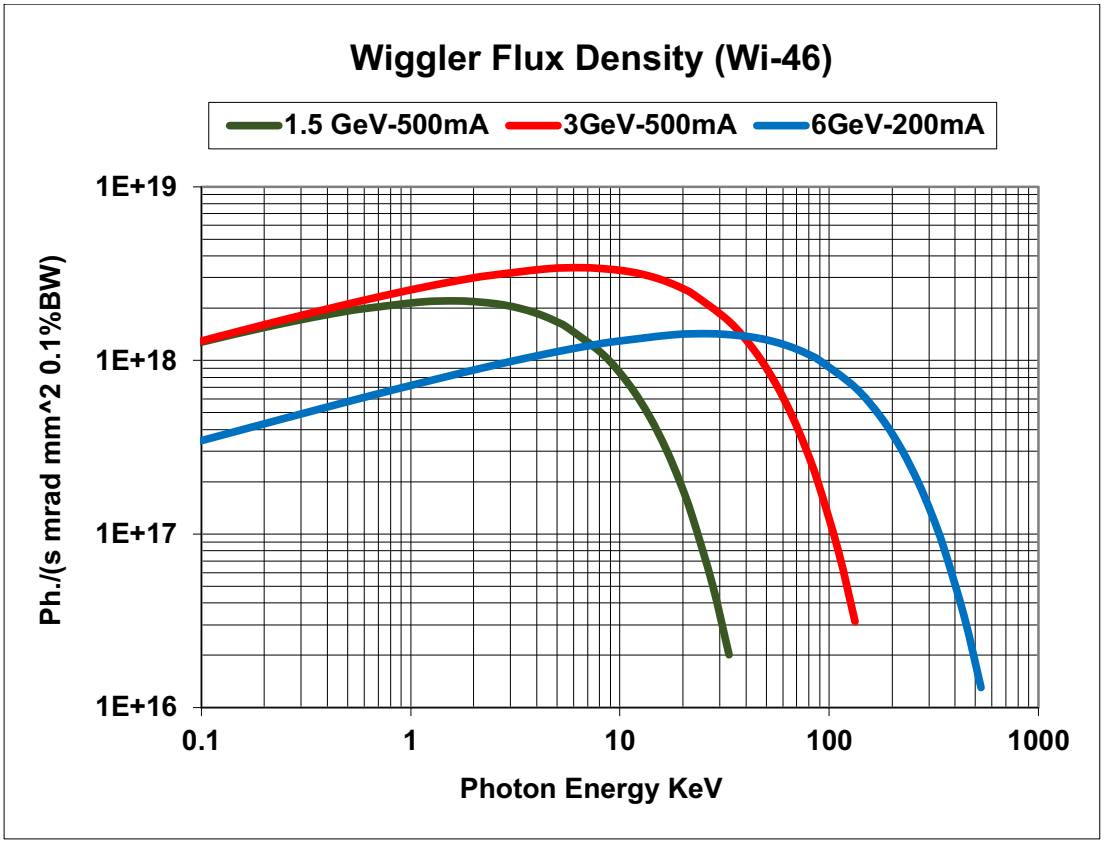

Fig. A.11: The radiation flux density of wiggler Wi-46 installed at SEE-LS for different energies and currents of 500 mA (1.5 GeV and 3 GeV) and 200 mA (6 GeV).

The wiggler flux density as a function of the photon energy is presented in Fig. A.11 for different electron beam energies. These characteristics are different from those of the bending magnet radiation because the emittance increases with the square of the beam energy and correspondingly the beam cross-section, as given in Table A.1.

The calculation of the brilliance of wigglers needs to take into account the depth of fields, i.e., the contribution to the apparent source size from different poles. The expression for the brilliance of the wigglers is

$$\mathrm{Br}_{\mathrm{Wiggler}} = \left\langle \frac{\mathrm{d}^2\Phi}{\mathrm{d}\theta\,\mathrm{d}\psi} \right\rangle (\psi = 0) \cdot \sum_{-N/2}^{N/2} \frac{1}{2\pi} \cdot \frac{\exp\left\{ -\frac{1}{2}\left(\frac{X_0^2}{\sigma_x^2 + z_n^2 \sigma_x'^2} \right) \right\}}{\left[\sigma_x^2 + z_n^2 \sigma_x'^2 \right]^{1/2} \left[\frac{\varepsilon_y^2}{\sigma_\psi^2} + \sigma_y^2 + z_n^2 \sigma_y'^2 \right]^{1/2}} \,. \tag{A.12}$$

where:

$$z_n = \lambda_\mathrm{p} \left(n + \frac{1}{4} \right) . \tag{A.13}$$

In Eq. (A.12) σ_x, σ_x', σ_y, and σ_y' are the r.m.s. transverse sizes and angular divergences of the electron beam at the centre of an insertion straight section ($\alpha_x = \alpha_y = 0$). This means that the brilliance of the wiggler calculated according to Eq. (A.12) is normalized to the middle of the straight section.

The exponential factor in Eq. (A.12) arises because the wigglers have two points, separated by $2X_0$ with X_0 as in Eq. (A.11). The sum in Eq. (A.12) goes over all poles of the wiggler. As already discussed in the section on the radiation of the bending magnets, the term $\varepsilon_y/\sigma_\psi$ is at least a factor of 10

smaller than the cross-section σ_y and so can be neglected. The expression $z_n\sigma_y^2$ is the increase of the source size from the centre of the insertion device.

Instead of normalizing the brilliance to the centre of the straight section, the cross-sections of the beam at the positions of the poles, $\sigma_x(n)$ and $\sigma_y(n)$, can be used, yielding a simpler expression for the brilliance:

$$\mathrm{Br}_{\mathrm{Wiggler}} = \left\langle \frac{\mathrm{d}^2\Phi}{\mathrm{d}\theta\,\mathrm{d}\psi} \right\rangle (\psi = 0) \cdot 2 \sum_{-N/2}^{N/2} \frac{1}{2\pi} \cdot \frac{\exp\left\{ -\frac{1}{2}\left(\frac{X_0^2}{\sigma_x^2(n)} \right) \right\}}{\sigma_x(n)\,\sigma_y(n)} \,. \tag{A.14}$$

The brilliances of the three types of wigglers in Table A.1 are presented in Fig. A.12. The brilliance is determined by the flux and the cross-sections of the beam; so because the cross-sections at the locations of the wigglers are three or four times larger than in the bending magnets, the brilliance of the wigglers is a factor of 20 more intense than that of the bending magnets.

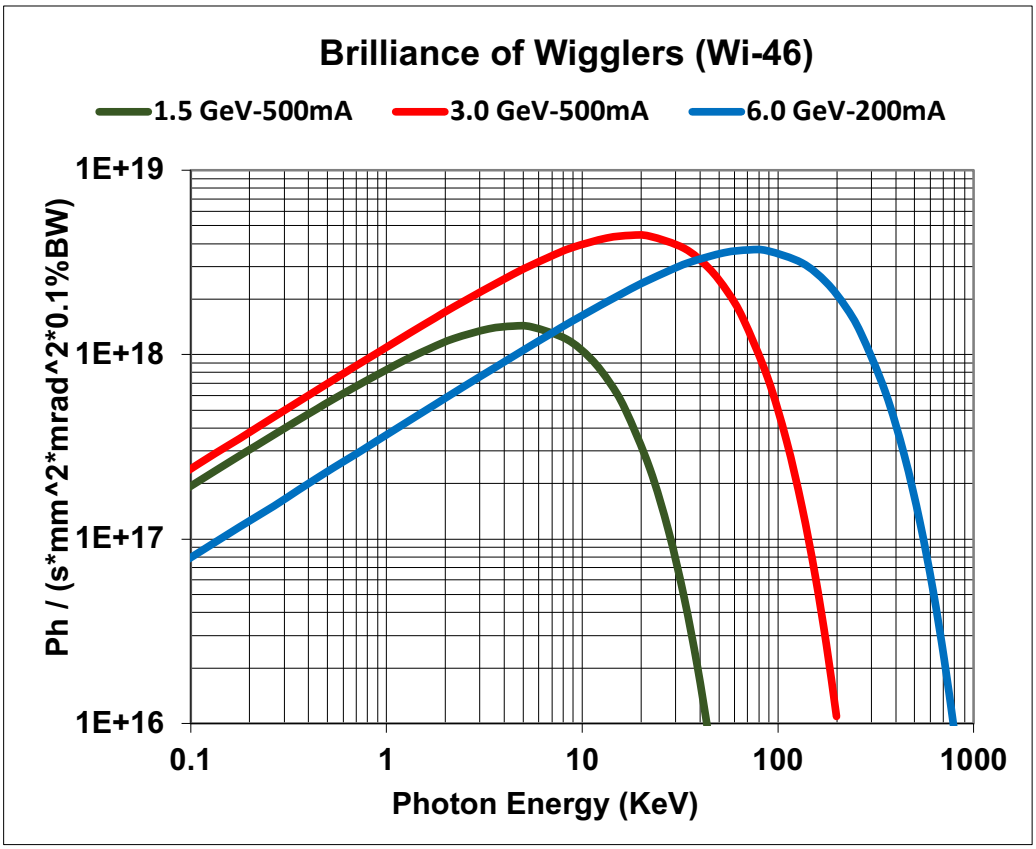

Fig. A.12: The radiation brilliance of the wiggler Wi-46 installed at SEE-LS for different energies and currents of 500 mA (1.5 GeV and 3 GeV) and 200 mA (6 GeV).

According to Eq. (A.14), the brilliance of a wiggler is inversely proportional to the cross-section of the beam and not to the emittance, because the amplitude X_0 of the beam oscillation has to be taken into account. In general the beam cross-section can be manipulated with the beta function in the storage ring. The dependence of the wiggler brilliance on the photon energy is shown in Fig. A.12 for different electron beam energies. The dependence on the beam energy is completely different from that of the bending radiation (cf. Fig. A.7), because the cross-sections are a function of the beam energy.

A.4 Radiation from an undulator

The opening angle σ_ψ of the synchrotron radiation from the bending magnet at the critical photon energy ε_c is, according to Eq. (A.5), about $0.655/\gamma$ or $1/\gamma$. The maximum slope of the electron trajectory in a wiggler is $X' = K / \gamma$. For values of K between 1 and 2, the deflection angle in a wiggler is within the opening angle of the synchrotron radiation [A.7–A.9]. In this special case the radiation from different periods interferes coherently, thus producing sharp peaks and resulting in completely different radiation characteristics. This radiation, as symbolized in Fig. A.13, is called undulator radiation, and the corresponding insertion devices are undulators. A photo of an insertion device is given in Fig. A.15.

Fig. A.13: Characterization of the undulator radiation; L is the period length of the undulator

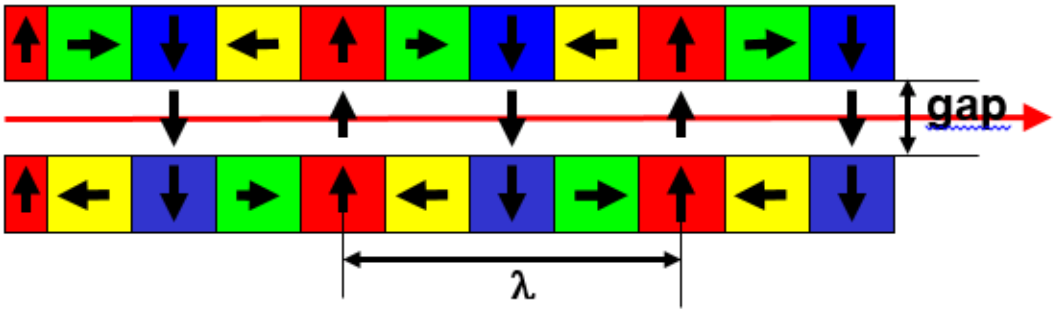

Fig. A.14: The arrangement of magnets within an undulator; the red, green, blue, and yellow blocks represent permanent magnets.

Undulators are insertion devices like the wigglers but with a smaller K values (between 1 and 2). The general set-up of an undulator is shown in Figs. A.14 and A.15. The blocks of different colours represent the permanent magnets, and the direction of the magnetic field is represented by arrows. The period length is denoted by λ.

The undulator emits radiation only at characteristic wavelengths:

$$\lambda_n = \frac{\lambda_{\mathrm{Und}}}{2n\gamma^2}\left(1+\frac{K^2}{2}+\gamma^2\Theta^2\right). \tag{A.15}$$

The corresponding photon energies are

$$\varepsilon_n = 0.949\ \mathrm{keV}\cdot(E/\mathrm{GeV})^2\,\frac{n}{(\lambda_{\mathrm{Und}}/\mathrm{cm})\left(1+(K^2/2)+\gamma^2\Theta^2\right)}\,, \tag{A.16}$$

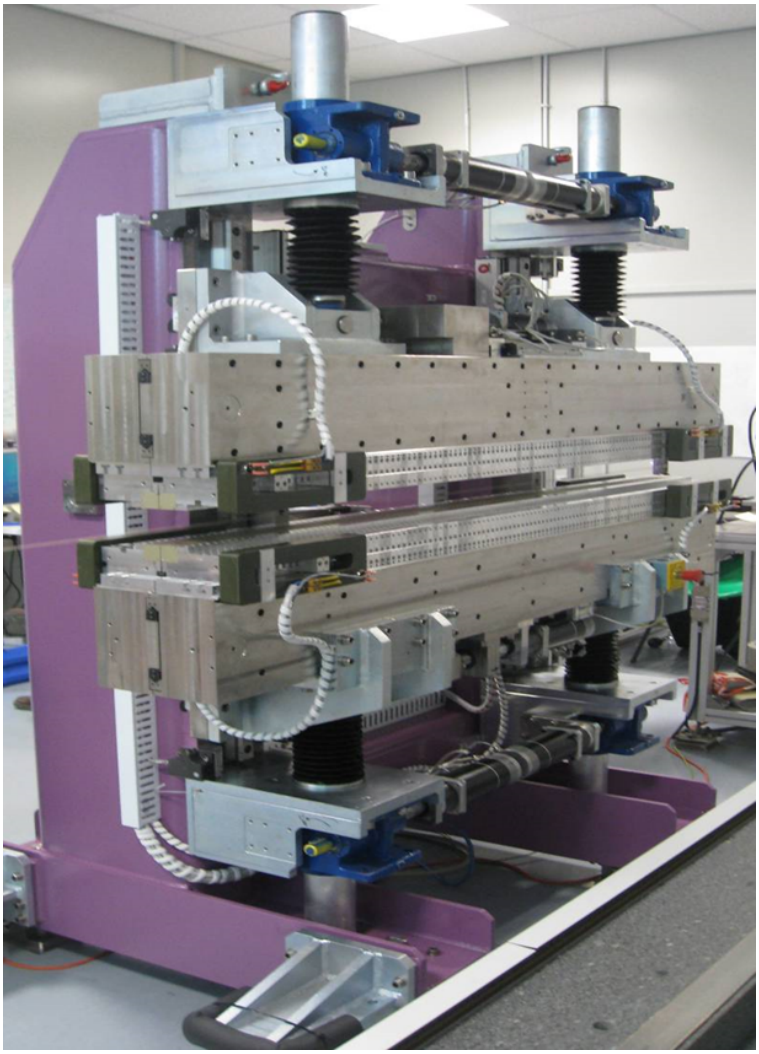

Figure A.15: Photo of an insertion device

with bandwidth

$$\frac{\Delta\varepsilon_n}{\varepsilon_n} = \frac{1}{n\,N_{\mathrm{Und}}}\ , \tag{A.17}$$

where:

n is the harmonic number (n = 1, 3, 5, 7, …);

N_{Und} is the number of periods;

λ_{Und} is the period length of the undulator;

K is the deflection parameter (see Eq. (A.11));

Θ is the observation angle in the horizontal direction.

The opening angle (σ'_γ) and the cross-section (σ_γ) of the undulator radiation are

$$\sigma_\gamma = \frac{\lambda_{\mathrm{Und}}}{4\pi\gamma}\sqrt{\frac{(1+K^2/2)N}{2n}},\quad \sigma'_\gamma = \frac{1}{\gamma}\sqrt{\frac{1+K^2/2}{2Nn}}\ . \tag{A.18}$$

The maximum slope X_0' and the amplitude X_0 characterizing the trajectory of the electron beam are

$$X_0 = \frac{1}{2\pi}\cdot\frac{K}{\gamma}\cdot\lambda_p = \frac{8.13\times10^{-5}}{(E/\mathrm{GeV})}K\lambda_p, \quad X_0' = \frac{K}{\gamma} = \frac{5.1\times10^{-4}K}{(E/\mathrm{GeV})} \ . \tag{A.19}$$

The K values for the undulators are roughly a factor of 10 smaller than for the wigglers; hence the amplitude X_0 and the divergence X_0' for the undulators are around a factor of 10 smaller than for the wigglers.

$\Delta\varepsilon_n/\varepsilon_n$ is the energy resolution of the spectral line emitted from the undulator. To reach the required bandwidth of 0.1%, the product of n and N must be at least 1000.

The following example (in-vacuum undulator) illustrates the characteristics of the undulator radiation.

The flux of the undulator radiation within the cone of the harmonics is given by (in practical units)

$$\Phi_{\mathrm{Und}}(n,K) = 1.432\times10^{14}\,N_{\mathrm{Und}}\cdot(I/\mathrm{A})\cdot Q_n(K)\,[\mathrm{photons/(s\ 0.1\%BW)}] \ . \tag{A.20}$$

According to Eq. (A.20), the flux of the undulator radiation is proportional to the number of periods, the current, and the function $Q_n(K)$ (see Fig. A.16). It is independent of the energy and the cross-section of the electron beam and is independent of the machine parameters. To reach a high photon flux (also for higher harmonics), the deflection parameter K should be in the range of 1 to 3. According to Eq. (A.16) the photon spectrum is proportional to the square of the energy and inversely proportional to the period length λ. In order to achieve X-ray radiation, the energy has to be in the range of 4–6 GeV with a period length of 40 mm. The gap would be 11 mm and the magnets of the undulator are outside the vacuum. Smaller period lengths can be attained only by reducing the gap, which is possible by putting the undulator inside the vacuum; so this type of undulator is called an 'in-vacuum undulator'. The smallest period lengths can be reached with superconducting magnets. These types of undulator are called 'mini-undulators'.

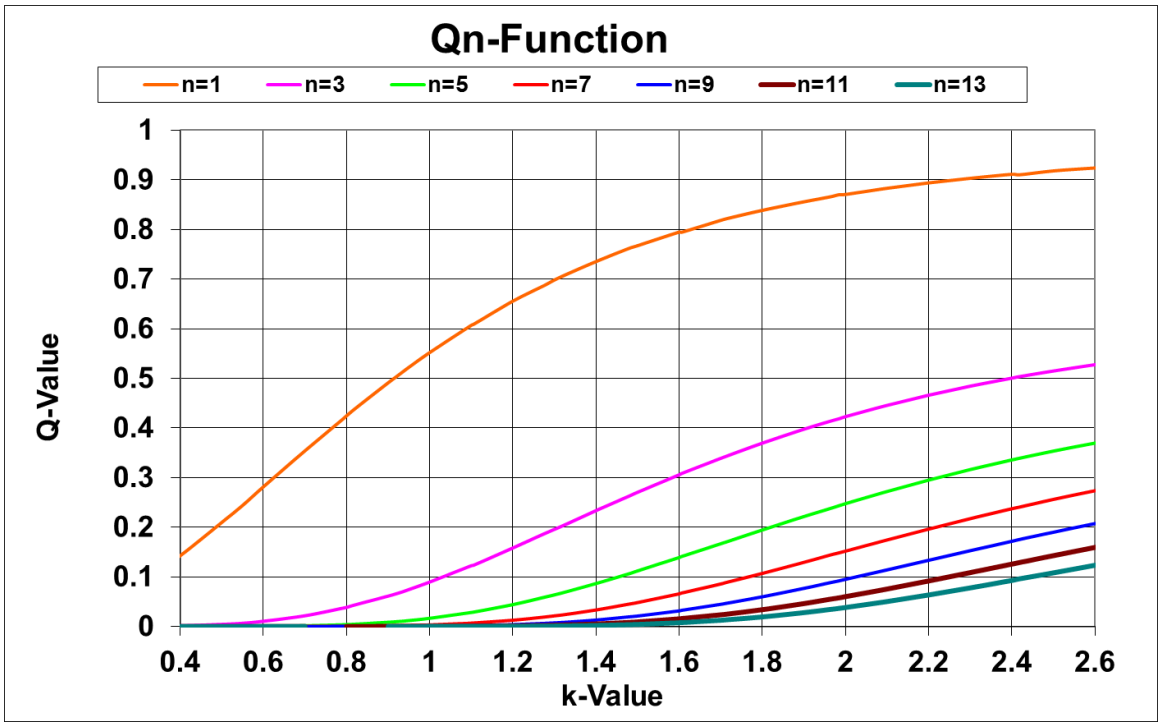

Fig. A.16: The dependence of the Q_n values on the K values

The photon flux of the MAX IV undulator with the specifications L = 2 m, λ = 15 m, and B_{max} = 1.5 T at an energy of 3 GeV and with a stored beam of 250 mA is presented in Fig. A.17.

The peak intensity on the axis of the nth harmonic of the undulator radiation is given by (in practical units of photons/(s mrad^{2}0.1%BW))

$$\frac{\mathrm{d}^2\Phi_{\mathrm{Und}}}{\mathrm{d}\theta\,\mathrm{d}\psi}(\theta=\psi=0)=1.744\times10^{14}\cdot N_{\mathrm{Und}}^2\cdot(E/\mathrm{GeV})^2(I/\mathrm{A})\cdot F_n(K)\ . \tag{A.21}$$

The peak intensity is proportional to the electron current, the radiation function $F_n(K)$ (see Fig. A.19), and the square of the period number. The opening angle of the radiation cone is inversely proportional to the energy, and therefore the peak intensity according to Eq. (A.21) is proportional to the square of the energy.

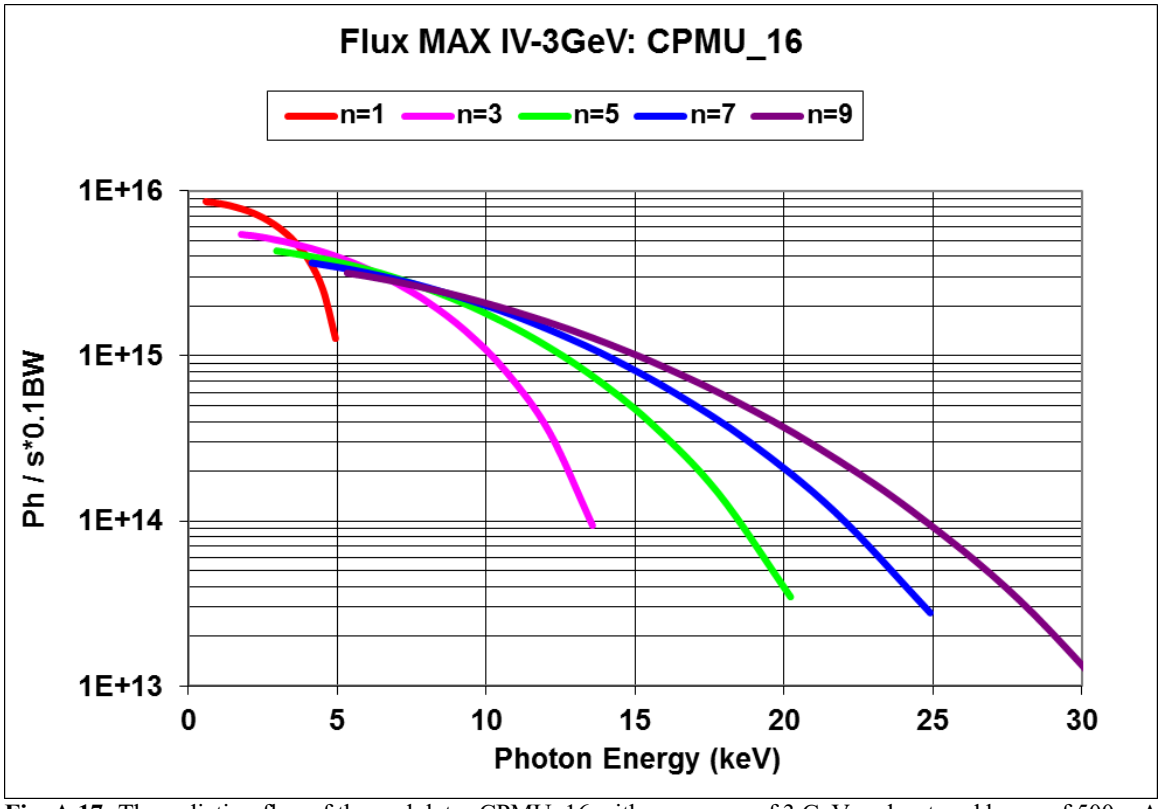

Fig. A.17: The radiation flux of the undulator CPMU_16 with an energy of 3 GeV and a stored beam of 500 mA calculated for the harmonics n = 1, 3, 5, 7, and 9. The period length of the undulator is 16 mm, the length is 2 m, and the maximum magnetic field is 1.5 T.

The brilliance of the undulator radiation is given by

$$\mathrm{Br}_{\mathrm{Und}}=\frac{\Phi_{\mathrm{Und}}(n,K)}{\left(2\pi\sum_x\sigma\sum_y\sigma\right)\left(2\pi\sum_x\sigma'\sum_y\sigma'\right)}\ , \tag{A.22}$$

with

$$\sum_x\sigma=\sqrt{\sigma_x^2+\sigma_r^2},\quad \sum_y\sigma=\sqrt{\sigma_y^2+\sigma_r^2},\quad \sum_x\sigma'=\sqrt{\sigma_x'^2+\sigma_r'^2},\quad \sum_y\sigma'=\sqrt{\sigma_y'^2+\sigma_r'^2}\ , \tag{A.23}$$

where

$$\sigma_{x,y}=\sqrt{\varepsilon_{x,y}\cdot\beta_{x,y}},\quad \sigma'_{x,y}=\sqrt{\varepsilon_{x,y}/\beta_{x,y}},\quad \sigma_r=\frac{1}{4\pi}\sqrt{\lambda L},\quad \sigma'_r=\sqrt{\lambda/L}\ . \tag{A.24}$$

Upon substituting λ from Eq. (A.15), σ_r and σ_r' are given by

$$\sigma_r = \frac{\lambda_{\mathrm{Und}}}{4\pi\gamma}\sqrt{\frac{(1+K^2/2)N}{2n}}, \quad \sigma_r' = \frac{1}{\gamma}\sqrt{\frac{(1+K^2/2)}{2nN}} \ . \tag{A.25}$$

For the aforementioned undulator the cross-sections σ_r and divergences σ_r' according to Eq. (A.24) are presented in Fig. A.18.

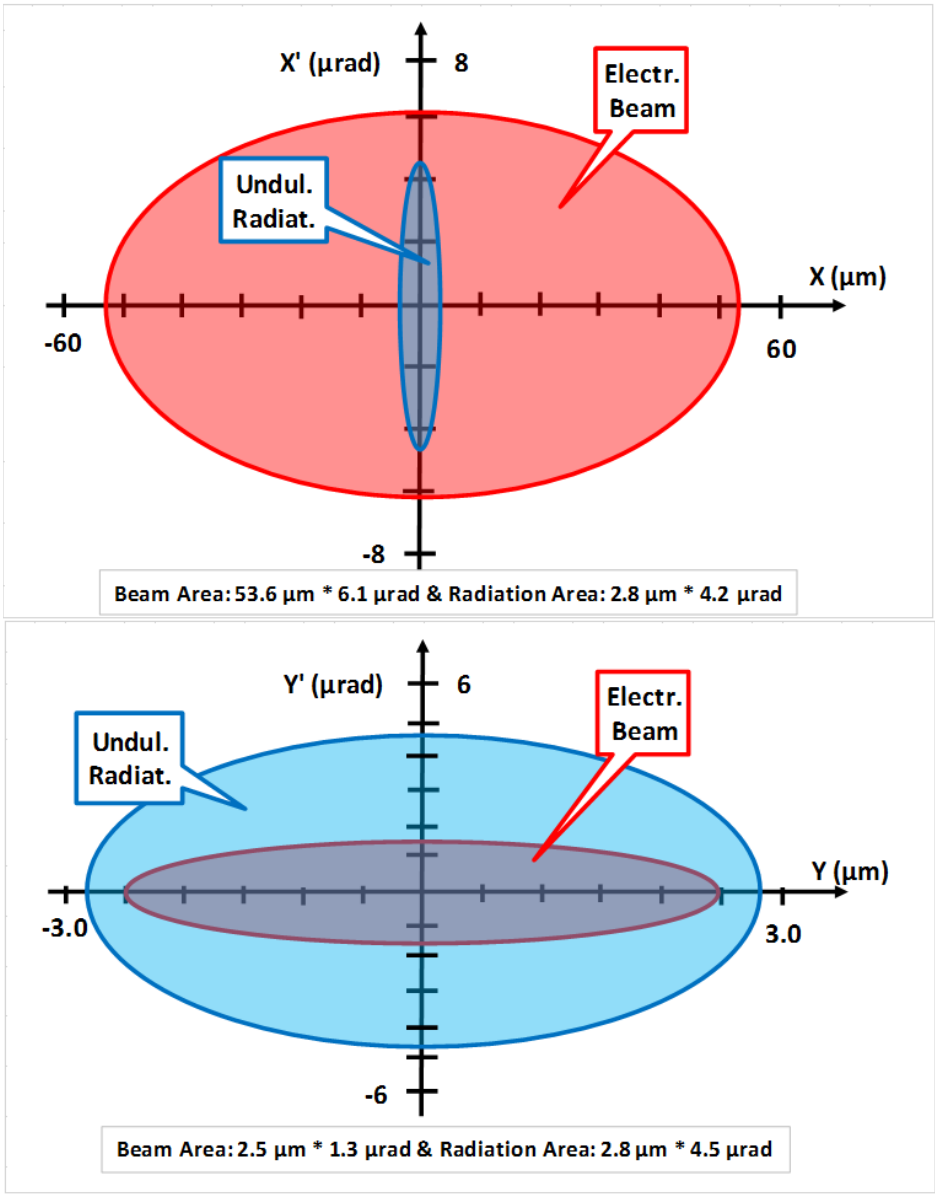

Fig. A.18: The phase space of the electron and radiation beam for the horizontal (upper diagram) and vertical (lower diagram) directions.

For the stored electron beam of 4th generation light sources such as MAX IV, the cross-sections and divergences are $\sigma_x \approx 54$ µm, $\sigma_y \approx 2.5$ µm, $\sigma_x' \approx 6.1$ µrad, $\sigma_y' \approx 1.3$ µrad, $\sigma_r \approx 2.8$ µm, and $\sigma_r' \approx 4.5$ µrad (see Fig. A.18). For the calculation of the brilliance, in the horizontal direction the wiggler radiation cone can be neglected, but in the vertical direction it has to be taken into account.

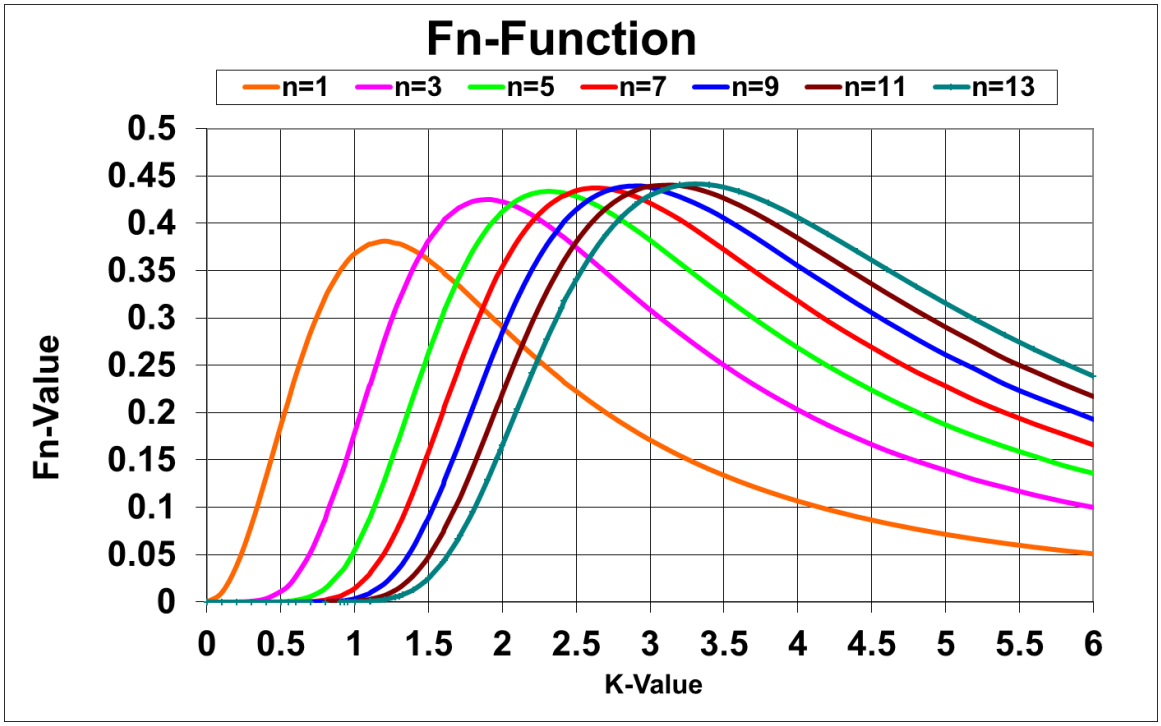

Fig. A.19: The dependence of the F_n values on the K values for the different harmonics

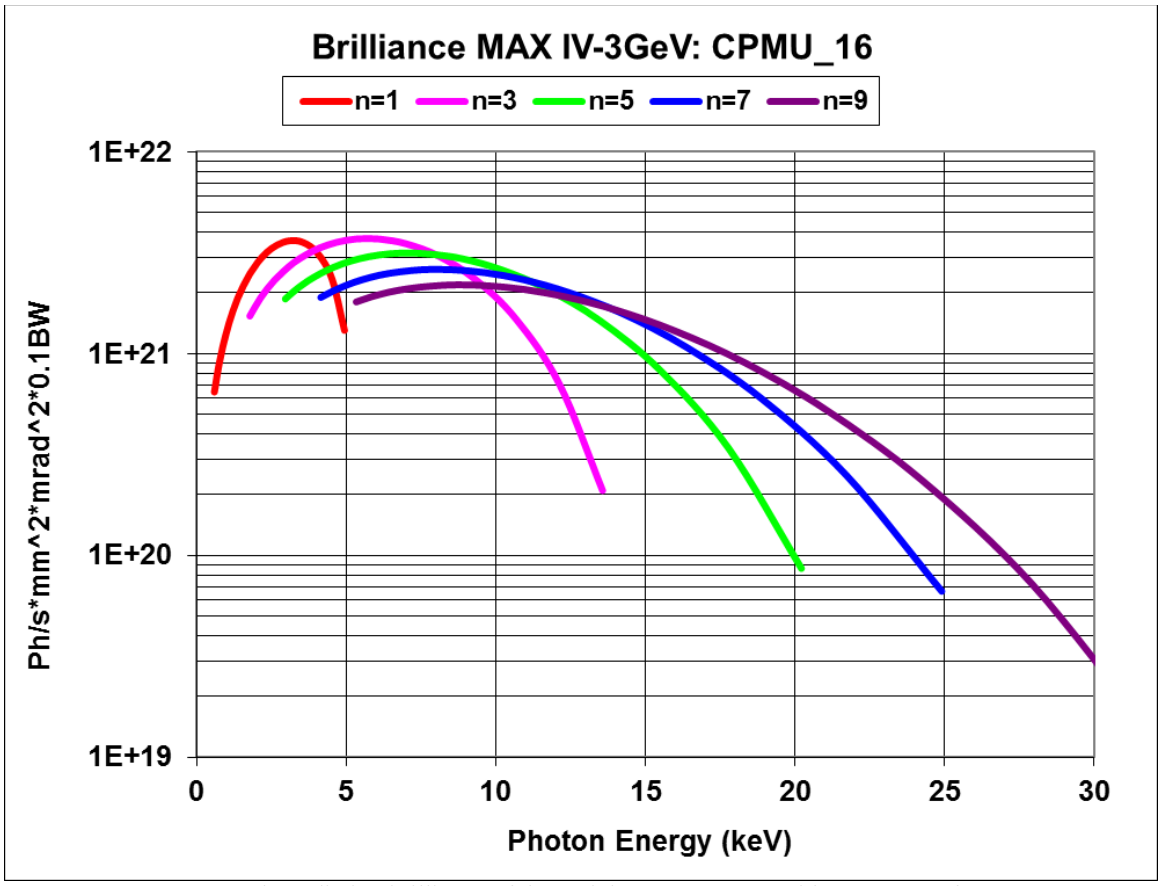

Fig. A.20: The radiation brilliance of the undulator CPMU_16 with an energy of 3 GeV

According to Fig. A.20, with a 4th generation light source such as MAX IV brilliances of up to 10^{22} photons/(s mm^2 mrad^2 0.1BW) can be reached.

A.5 Influence of the beam energy spread on the spectral photon flux

The spectral photon flux is the number of photons per second per 0.1% bandwidth. The bandwidth of the undulator radiation is given by Eq. (A.17). The dependence of the emitted photon spectrum on the energy is described by Eq. (A.16). According to the energy spread of the stored electrons, the electrons emit light with different energies. The relative energy spread ($\delta E/E$) of the stored electron beam is in the range of 10^{-3}. This gives an energy spread for the undulator radiation of $\delta E/E = 2 \times 10^{-3}$. For the aforementioned example we have the following results.

– Natural photon energy spread of undulator radiation:
$$\Delta\varepsilon_1 = 16.74 \text{ eV}, \Delta\varepsilon_3 = 16.74 \text{ eV}, \Delta\varepsilon_5 = 16.74 \text{ eV}, \ldots, \Delta\varepsilon_{11} = 16.74 \text{ eV}.$$

– Photon energy spread according to variation of the beam energy:
$$\delta\varepsilon_1 = 3.2 \text{ eV}, \delta\varepsilon_3 = 9.6 \text{ eV}, \delta\varepsilon_5 = 16 \text{ eV}, \delta\varepsilon_7 = 22.6 \text{ eV}, \delta\varepsilon_9 = 29 \text{ eV}, \ldots, \delta\varepsilon_{11} = 35.0 \text{ eV}.$$

According to these results, the spectral photon fluxes of the higher harmonics of the undulator radiation are determined by the energy spread of the stored electron beam. With this example it starts at the 5th harmonic. This has to be taken into account.

References

[A.1] H. Wiedemann, *Synchrotron Radiation* (Springer, Berlin, 2003), https://doi.org/10.1007/978-3-662-05312-6

[A.2] R. Walker, Synchrotron radiation, CAS-CERN Accelerator School: 5th General Accelerator Physics Course, Jyväskylä, Finland, 7–18 September 1992, CERN-1994-001 (CERN, Geneva, 1994), p. 437. https://doi.org/10.5170/CERN-1994-001

[A.3] CAS-CERN Accelerator School: Synchrotron Radiation and Free Electron Lasers, Grenoble, France, 22–27 April 1996, CERN-1998-004 (CERN, Geneva, 1998). https://doi.org/10.5170/CERN-1998-004

[A.4] H. Onuki and P. Elleaume, *Undulators, Wigglers and Their Applications* (Taylor and Francis, London, 2003), https://doi.org/10.4324/9780203218235

[A.5] J.A. Clarke, *The Science and Technology of Undulators and Wigglers* (Oxford University Press, Oxford, 2004), https://doi.org/10.1093/acprof:oso/9780198508557.001.0001

[A.6] J. Schwinger, *Phys. Rev.* **75** (1949) 1912, https://doi.org/10.1103/PhysRev.75.1912

[A.7] R. Walker, Insertion devices: undulators and wigglers, CAS-CERN Accelerator School: Synchrotron Radiation and Free Electron Lasers, Grenoble, France, 22–27 April 1996, CERN-1998-004 (CERN, Geneva, 1998), p. 129. https://doi.org/10.5170/CERN-1998-004

[A.8] L. Rivkin, Synchrotron radiation, CAS-CERN Accelerator School: FELs and ERLs, Hamburg, Germany, June 2014. (Proceedings not published.)
Lecture part I:
https://web.archive.org/web/20190514093703/http://cas.web.cern.ch/sites/cas.web.cern.ch/files/lectures/hamburg-2016/rivkiniii.pdf
Lecture part II:
https://web.archive.org/web/20190514093703/http://cas.web.cern.ch/sites/cas.web.cern.ch/files/lectures/hamburg-2016/rivkiniii.pdf

[A.9] J. Pflueger, Undulator technology, CAS-CERN Accelerator School: FELs and ERLs, Hamburg, Germany, June 2014. (Proceedings not published.)
Lecture:
https://web.archive.org/web/20190514094217/http://cas.web.cern.ch/sites/cas.web.cern.ch/files/lectures/hamburg-2016/pflueger.pdf